Investigating the coalescence-inspired sum rule for light nuclei and hypernuclei in heavy-ion collisions

Ashik Ikbal Sheikh ⊙*

Department of Physics, Kent State University, Kent, Ohio 44242, USA

A data-driven idea is presented to test if light nuclei and hypernuclei obey the coalescence-inspired sum rule, i.e., to test if the flow of a light nucleus or hypernucleus is the summed flow of each of its constituents. Here, the mass difference and charge difference among the constituents of light nuclei and hypernuclei are treated appropriately. The idea is applied to the available data for $\sqrt{s_{NN}} = 3$ GeV fixed-target Au+Au collisions at the Relativistic Heavy Ion Collider (RHIC), published by the STAR Collaboration. It is found that the sum rule for light nuclei is approximately valid near midrapidity ($-0.3 < y < 0$), but there is a clear violation of the sum rule at large rapidity ($y < -0.3$). The Jet AA Microscopic Transport Model (JAM), with baryonic mean-field plus nucleon coalescence, generates a similar pattern as obtained from the experimental data. In the present approach, the rapidity dependence of directed flow of the hypernuclei $^3_\Lambda$H and $^4_\Lambda$H is predicted in a model-independent way for $\sqrt{s_{NN}} = 3$ GeV Au+Au collisions, which will be explored by ongoing and future measurements from STAR.

I. INTRODUCTION

Collectivity is a phenomenon observed over a wide range of collision energies for various heavy-ion collision systems. The azimuthal anisotropy of emitted particles is characterized by Fourier decomposition of final-state particle momenta with respect to the reaction plane [1,2]. The first- and higher-order coefficients of the azimuthal anisotropy, also known as directed flow (v_1), anisotropic flow (v_2), and so on, describe a collective motion of particles. The azimuthal anisotropies provide important information on the collective hydrodynamic expansion and transport properties of the matter formed in the collisions. They are also sensitive to the compressibility of the nuclear matter and the nuclear equation of state at collision energies of the order of a few GeV [3,4]. The anisotropic flow coefficients of different identified particle species have been measured extensively in experiments at RHIC [5–9] and the LHC [10,11].

Apart from the identified particles, the measurements of hypernuclei ($^3_\Lambda$H, $^4_\Lambda$H) [12–16] and measured azimuthal anisotropies for light nuclei (d, t, ^{3}He, ^{4}He) [17–26] have also been reported in the past. Hypernuclei are natural hyperon-baryon correlation systems, and can serve as an excellent probe of hyperon-baryon interactions in high-energy heavy-ion collisions. Measurements of hypernuclei produced in the collisions have lately been of increasing interest. On the other hand, at lower collision energies, a larger anisotropic flow is measured for light nuclei compared to protons [19–25,27,28], suggesting possible advantages of studying light nuclei. The STAR Collaboration reported the scaling of light nuclear elliptic flow according to nuclear mass number (A), in a reduced

transverse momentum (p_T) range $p_T/A < 1.5$ GeV/c over a wide range of collision energies, $\sqrt{s_{NN}} = 7.7$–200 GeV [24]. This observation favors the interpretation that the light nuclei are formed at these energies and kinematics via coalescence of nucleons. However, the true production mechanism of light nuclei and hypernuclei is not yet fully understood and remains under active research [29–33]. In the coalescence mechanism, light nuclei or hypernuclei are formed by the binding of nucleons or hyperons when they come close to each other in both coordinate and momentum space during the time of kinetic freezeout [34–36]. The interaction between the produced expanding fireball and the spectator remnants becomes more significant at lower beam energies due to the longer passing time of the colliding ions. The flow signals are strongly affected by the relatively slowly passing spectators, and hence one might get important insights into the collision dynamics and the nucleon coalescence behavior. Recently, the STAR Collaboration has observed a breakdown of A scaling for flow of light nuclei away from midrapidity in $\sqrt{s_{NN}} = 3$ GeV Au+Au collisions [28].

In the traditional A scaling for light nuclei and hypernuclei (e.g., Ref. [28]), each constituent nucleon or hyperon is on equal footing, which ignores the fact that the constituents have different masses and electric charges, whereas the resulting flow of nuclei through coalescence mechanism depends on the mass and charge of the constituents. The mass difference between proton and neutron may be negligibly small, but due to the charge difference, the Coulomb effect must be larger than the mass effect. In this paper, a novel data-driven method is discussed, which tests the coalescence-inspired sum rule for light nuclei and hypernuclei, considering different constituents according to their mass and charge.

It is hard to measure each and every constituent of a light nucleus or hypernucleus in an experiment. Hence, the idea is

---

*asheikh2@kent.edu; ashikhep@gmail.com

to combine different light nuclei and hypernuclei, then compare the combinations so that they have identical constituents, i.e., the combinations are compared at the same mass and same charge at the constituent level. The method is discussed in detail in the next section (Sec. II). Under this method, the sum rule is tested using the STAR measurements available for light nuclei from $\sqrt{s_{NN}} = 3$ GeV Au+Au collisions. A nuclear transport model named the Jet AA Microscopic Transport Model (JAM) [37] with a baryonic mean-field [38] plus nucleon coalescence calculations is found to be quite successful in describing the measured v_1 and v_2 for light nuclei from $\sqrt{s_{NN}} = 3$ GeV Au+Au collisions [28]. The sum rule has also been tested with the same JAM model and the calculations agree with the results obtained from the STAR data at $\sqrt{s_{NN}} = 3$ GeV Au+Au collisions.

The data-driven method predicts the rapidity dependence of v_1 for hypernuclei such as $^3_\Lambda$H and $^4_\Lambda$H in $\sqrt{s_{NN}} = 3$ GeV Au+Au collisions. STAR has collected large data sets at various beam energies, both in fixed target and collider modes as part of Phase II of the Beam Energy Scan program [39], and these detailed measurements will serve as a good testing ground for the analysis proposed in the present work.

In the next section, details of the method are outlined. Results are discussed in Sec. III. Section IV presents a summary.

II. METHOD

A. Coalescence-inspired sum rule in a data-driven approach

In the proposed approach, it is assumed that light nuclei and hypernuclei are predominantly formed via coalescence of the constituent nucleons or Λ hyperons, and it is also assumed that the anisotropic flow correlation is imposed before hadronization [12,24], i.e., well before formation of the nuclei under consideration. The abundantly produced light nuclei and hypernuclei reported by experimental collaborations to date are $d(pn)$, $t(pnn)$, ^{3}He(ppn), ^{4}He($ppnn$), $^3_\Lambda$H($pn\Lambda$), and $^4_\Lambda$H($pnn\Lambda$). The A scaling for light nuclei and hypernuclei follows from the coalescence mechanism. The different constituents of light nuclei and hypernuclei in this scaling behavior are treated equally, which ignores the fact that in general, the constituents have different masses, charges, and strangeness. In the following method, the coalescence-inspired sum rule for light nuclei and hypernuclei can be tested where the constituents are considered depending upon their masses, charges, and strangeness, i.e., the method does not ignore the mass difference, charge difference, and strangeness difference of the constituents. A similar approach was developed in earlier work [40], which focused on hadron formation via coalescence in heavy-ion collisions.

The first step in the present method is to select a kinematic region where the aforementioned assumptions of the sum rule can be tested, which involves a test of the equality

$$v_1(\text{light (hyper)nucleus}) = \sum_i v_1(N_i), \qquad (1)$$

where the sum runs over the v_1 for the nucleon or Λ hyperon constituents, N_i.

The next step of the method is to combine different light nuclei and hypernuclei, then compare the combinations,

TABLE I. Differences between the combinations formed from various light nuclei and hypernuclei. Each index represents a difference of two combinations with identical constituents, i.e., for all cases, the constituent-level mass difference is $\Delta m = 0$, the charge difference is $\Delta q = 0$, and the mass number difference is $\Delta A = 0$. Not all indices shown here are linearly independent. A set of linearly independent combinations can be found using linear algebra; one possible such set is 1, 2, 3, 6, and 7.

Index	Δv_1 combination
1	$p(p) + d(pn) - {}^3\text{He}(ppn)$
2	$p(p) + t(pnn) - {}^4\text{He}(ppnn)$
3	$d(pn) - \frac{1}{2}\,{}^4\text{He}(ppnn)$
4	$d(pn) + {}^3\text{He}(ppn) - p(p) - {}^4\text{He}(ppnn)$
5	$t(pnn) + {}^3\text{He}(ppn) - d(pn) - {}^4\text{He}(ppnn)$
6	${}^3_\Lambda\text{H}(pn\Lambda) - d(pn) - \Lambda(\Lambda)$
7	${}^4_\Lambda\text{H}(pnn\Lambda) - t(pnn) - \Lambda(\Lambda)$

which have identical constituents, i.e., the combinations being compared have the same mass and same charge at the constituent level. For example, $p(p) + d(pn)$ has the identical constituent nucleons as ^{3}He(ppn). Therefore, the consistency of the sum rule can be investigated experimentally by testing the equality

$$v_1[p(p)] + v_1[d(pn)] = v_1[^3\text{He}(ppn)]. \qquad (2)$$

Here, both left and right sides have the identical constituent nucleon content of ppn. Hence at the constituent level, the mass difference, the charge difference, and the mass number difference between left and right sides are $\Delta m = 0$, $\Delta q = 0$ and $\Delta A = 0$, respectively. However, the three nucleons here are distributed differently within the two light nuclei on the left side. For convenience of discussion, such combinations are expressed in terms of a difference, Δv_1. For example, Eq. (2) can be written as

$$\Delta v_1(\Delta m = 0,\ \Delta q = 0,\ \Delta A = 0)$$
$$= v_1[p(p)] + v_1[d(pn)] - v_1[^3\text{He}(ppn)]. \qquad (3)$$

Different terms in Eqs. (2) and (3) should be evaluated in a common region of rapidity $y_{\min} \leqslant y \leqslant y_{\max}$ and transverse momentum per constituent nucleon $(p_T/A)_{\min} \leqslant p_T/A \leqslant (p_T/A)_{\max}$. A common $y - p_T/A$ region is required if the coalescence mechanism is applicable. In other words, if one measures v_1 of p, d, and ^{3}He in $y_{\min} \leqslant y \leqslant y_{\max}$ as a function of transverse momentum p_T^p, p_T^d and $p_T^{3\text{He}}$, respectively, then Eq. (3) should be evaluated in the kinematic region where $(p_T/A)_{\min} < (p_T^p),\ (p_T^d/2),\ (p_T^{3\text{He}(ppn)}/3) < (p_T/A)_{\max}$.

Similar to the combinations in Eq. (3), various combinations are arranged in Table I where each index represents a difference between two combinations having identical constituents. The sum rule can be investigated experimentally in a model-independent way by each index as shown in Table I. The result given by any of the indices can be cross checked by other indices. Indices 1–5 are constructed from light nuclei only whereas index 6 and index 7 contain hypernuclei ($^3_\Lambda$H and $^4_\Lambda$H) along with nonstrange light nuclei. In indices 6 and 7, the Λ hyperon is balanced in such a way that the net

TABLE II. The vectors constructed from each combination in Table I. These vectors are formulated in the $\mathbf{R}^8$ vector space where the basis is formed by the light nuclei and hypernuclei discussed here, namely, p, d, t, $^3\mathrm{He}$, $^4\mathrm{He}$, Λ, $^3_\Lambda\mathrm{H}$, and $^4_\Lambda\mathrm{H}$.

Index	Δv_1 combination	Vector
1	$p(p) + d(pn) - {}^3\mathrm{He}(ppn)$	$v_1 = \{1, 1, 0, -1, 0, 0, 0, 0\}$
2	$p(p) + t(pnn) - {}^4\mathrm{He}(ppnn)$	$v_2 = \{1, 0, 1, 0, -1, 0, 0, 0\}$
3	$d(pn) - \frac{1}{2}\,{}^4\mathrm{He}(ppnn)$	$v_3 = \{0, 1, 0, 0, -1/2, 0, 0, 0\}$
4	$d(pn) + {}^3\mathrm{He}(ppn) - p(p) - {}^4\mathrm{He}(ppnn)$	$v_4 = \{-1, 1, 0, 1, -1, 0, 0, 0\}$
5	$t(pnn) + {}^3\mathrm{He}(ppn) - d(pn) - {}^4\mathrm{He}(ppnn)$	$v_5 = \{0, -1, 1, 1, -1, 0, 0, 0\}$
6	$^3_\Lambda\mathrm{H}(pn\Lambda) - d(pn) - \Lambda(\Lambda)$	$v_6 = \{0, 1, 0, 0, 0, 1, -1, 0\}$
7	$^4_\Lambda\mathrm{H}(pnn\Lambda) - t(pnn) - \Lambda(\Lambda)$	$v_7 = \{0, 0, 1, 0, 0, 1, 0, -1\}$

strangeness, ΔS, is also zero. It is indeed very interesting to investigate the charge and strangeness dependence of the sum rule by constructing similar combinations having same or similar mass at the constituent level but different electric charge and strangeness. However. this is beyond scope of this paper.

The proposed experimental test of the sum rule for light nuclei and hypernuclei can be applied to a variety of collision systems at a wide range of collision energies. The sum rule test can also be applied to other flow harmonics, such as v_2. It is to be noted here that the present method tests the simplified version of the sum rule where the light nucleus or hypernucleus v_1 is the simple addition of its constituents v_1. However, corrections for higher-order terms in the sum rule might be important when the v_1 magnitude is sufficiently larger. One should keep in mind that the higher-order terms contain $v_1(n)$, which cannot be measured in experiment. The higher-order corrections are not included in the present work.

Section III applies the proposed method to light nuclei in $\sqrt{s_{NN}} = 3$ GeV Au+Au collisions from STAR. At present, there are no published anisotropic flow measurements for $^3_\Lambda\mathrm{H}$ and $^4_\Lambda\mathrm{H}$ in $\sqrt{s_{NN}} = 3$ GeV Au+Au collisions. Therefore, the sum rule cannot be investigated for indices 6 and 7 at this time. Indices 6 and 7 can be exploited to predict the v_1 of $^3_\Lambda\mathrm{H}$ and $^4_\Lambda\mathrm{H}$ in $\sqrt{s_{NN}} = 3$ GeV Au+Au collisions:

$$v_1[^3_\Lambda\mathrm{H}(pn\Lambda)] = \Delta v_1 + v_1[d(pn)] + v_1[\Lambda(\Lambda)], \quad (4)$$

$$v_1[^4_\Lambda\mathrm{H}(pnn\Lambda)] = \Delta v_1 + v_1[t(pnn)] + v_1[\Lambda(\Lambda)], \quad (5)$$

where Δv_1 is the difference in v_1 between identical constituent combinations. The Δv_1 is the measure of the sum rule check. In an ideal scenario where the sum rule holds, Δv_1 should be zero. In this case, a global Δv_1 is obtained by fitting the Δv_1 calculations from other indices of Table I. One should fit the Δv_1 from a set of independent indices only. The indices of Table I are not all linearly independent. A set of linearly independent indices can be found by employing linear algebra as discussed in Sec. II B.

B. Evaluation of linearly independent combinations

This section is dedicated to figuring out the linearly independent light nuclei and hypernuclei combinations as presented in Table I. There are six independent measurements (v_1 of Λ, p, d, t, $^3\mathrm{He}$, and $^4\mathrm{He}$), using them seven combinations are made up (see Table I), and hence each combination must

not be independent. A set of linearly independent combinations is necessary to estimate the global Δv_1 which is useful to get an overall estimation of the sum rule test and predict v_1 of $^3_\Lambda\mathrm{H}$ and $^4_\Lambda\mathrm{H}$ [see Eqs. (4) and (5)]. The global Δv_1 can be obtained by fitting the Δv_1 measurements of the independent combinations. To make the fit reliable, one has to use the independent data points in the fitting. Because any sort of correlations among the fitted data points can make the fitting procedure biased.

To find sets of linearly independent combinations among the seven combinations, linear algebra is employed where the present problem is mapped into a linear vector space. The same method of linear algebra was used to identify independent hadron combinations in a previous work [40]. Here, it is assumed that light nuclei and hypernuclei along with the Λ hyperon used in this approach form a basis $B = \{ p, d, t, {}^3\mathrm{He}, {}^4\mathrm{He}, \Lambda, {}^3_\Lambda\mathrm{H}, {}^4_\Lambda\mathrm{H} \}$ of a eight-dimensional vector space, $\mathbf{R}^8$, where the elements of B are called basis vectors in this space. This assumption is well justified since the experimental measurements of v_1 of each light nucleus, hypernucleus, Λ hyperon are independent and can represent independent basis vectors of a vector space. All the combinations or indices made up from them are vectors in that space ($\mathbf{R}^8$), and together constitute a set of vectors, $V = \{v_1, v_2, \ldots, v_r\}$, where r is the total number of vectors in the set (in this case $r = 7$). The vectors for all the combinations are presented in Table II.

The set of vectors, $V = \{v_1, v_2, \ldots, v_r\}$ is linearly dependent if there exists a set of nonzero scalars $(\beta_1, \beta_2, \ldots, \beta_r)$ such that

$$\sum_{i=1}^{r} \beta_i v_i = \mathbf{0}, \quad (6)$$

where $\mathbf{0}$ is a null vector in the same space. In other words, the vectors are linearly dependent if at least one vector can be expressed as a linear combination of the others. The vectors in V are linearly independent when all the coefficients in Eq. (6) are zero [41].

Each vector of V can be represented as a column matrix of dimension 8×1, where 8 is the dimension of the vector space in the present case. This implies that Eq. (6) is a matrix equation where the seven vectors together form a matrix, M, of dimension 8×7 and the scalars $\beta_1, \beta_2, \ldots, \beta_7$ constitute a column matrix, B, with dimensions 7×1, i.e.,
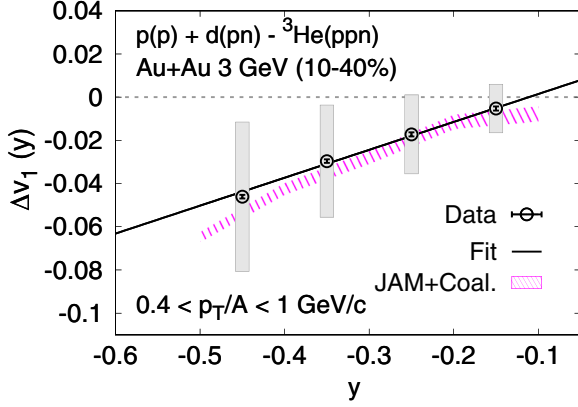
$$MB = O, \quad (7)$$

FIG. 1. Calculations of Δv_1 based on index 1 (see Table I) for $\sqrt{s_{NN}} = 3$ GeV Au+Au collisions at 10–40 % centrality, where the v_1 of ^{3}He(ppn) is subtracted from the combined v_1 of $p(p)$ and $d(pn)$ as shown in Eq. (3). $p(p) + d(pn)$ has the same nucleon content as ^{3}He(ppn). Experimental measurements as well as the JAM (mean-field)+coalescence calculations of v_1 are taken from Ref. [28].

where O is a null matrix of dimensions 8×1. The matrix M should be expressed in row-reduced echelon form by several row and column operations to solve the matrix equation, Eq. (7). At the end, Eq. (7) with the row-reduced form of M evaluates the scalars $\beta_1, \beta_2, \ldots, \beta_7$.

Employing the above method of linear algebra, it is found that the seven indices of Table I are not linearly independent. Therefore, the number of vectors in the set V can be reduced repeatedly until an independent vector subset is identified. The five indices 1, 2, 3, 6, and 7 are thus found to be linearly independent. Note that other sets of independent combinations can exist.

III. RESULTS AND DISCUSSIONS

The proposed method to test the coalescence sum rule for light nuclei is applied to the STAR experimental data for $\sqrt{s_{NN}} = 3$ GeV Au+Au collisions. The JAM model with baryonic mean field plus nucleon coalescence calculations

are quite successful in describing the measured v_1 and v_2 for light nuclei from $\sqrt{s_{NN}} = 3$ GeV Au+Au collisions [28]. Therefore, the findings obtained from the experimental data and the model are expected to be consistent. The JAM model + coalescence can provide further understanding of light nucleus formation, the coalescence-inspired sum rule, and scaling behavior. The JAM model simulates nucleon production from the initial collision phase to the final hadron transport in Au+Au collisions. In the mean-field mode of this model [38], nucleon evolution is performed by using a momentum-dependent potential with the incompressibility parameter, $\kappa = 380$ MeV. To simulate light nuclei, the JAM mean-field mode employs a coalescence afterburner at a fixed time of 50 fm/c. Each nucleon pair is boosted to the rest frame, then the relative position (Δr) and relative momentum (Δp) determines whether a light nucleus is formed. For example, if $\Delta r < 4$ fm and $\Delta p < 0.3$ GeV/c, then the nucleon pair is tagged as a $d(pn)$ [42]. Other light nuclei with $A > 2$, such as $t(pnn)$, ^{3}He(ppn), and ^{4}He($ppnn$), are formed by adding up the constituent nucleons one by one as per the Δr and Δp values in the rest frame. For more details of the model calculations, see Ref. [28].

Figure 1 presents estimates of Δv_1 [Eq. (3)] as a function of rapidity, y, for $\sqrt{s_{NN}} = 3$ GeV Au+Au collisions at 10–40 % centrality. Δv_1 is calculated by subtracting the v_1 of ^{3}He(ppn) from the combined v_1 of $p(p)$ and $d(pn)$ as described by index 1 in Table I. The calculations are performed in a common region of $y - p_T/A$ space, $-0.5 < y < 0$ and $0.4 < p_T/A < 1$ GeV/c, using the v_1 measurements for light nuclei reported by STAR [28]. Calculations from JAM mean field with coalescence are also shown here. Especially near midrapidity, $-0.3 < y < 0$, Δv_1 is roughly consistent with zero within the measured error bars, indicating that the sum rule is followed approximately. However, moving away from midrapidity ($y = 0$), Δv_1 magnitudes increase gradually and deviate from zero. This implies a sum rule violation, which is more prominent at larger rapidity magnitudes ($y < -0.3$). The JAM mean-field with coalescence calculations agree with the data-driven calculations within uncertainties and hence exhibit a similar violation of the sum rule.
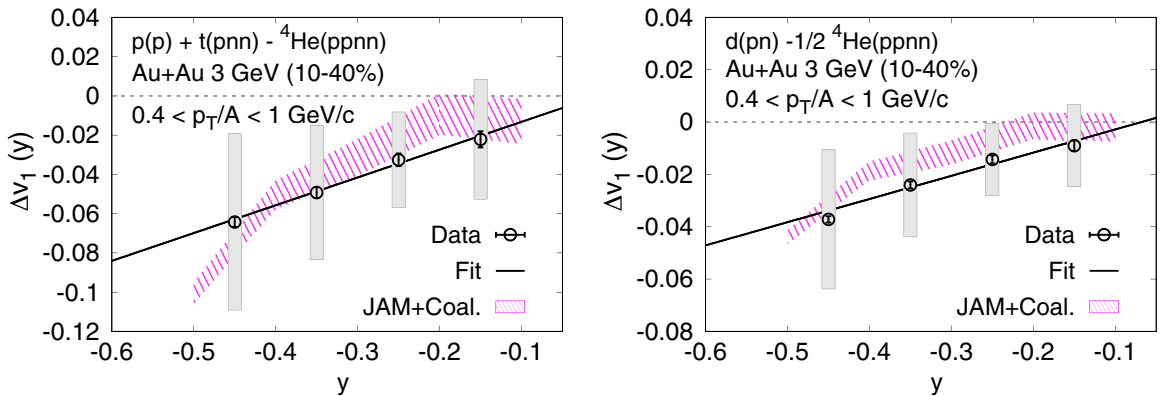

FIG. 2. Calculations of Δv_1 based on index 2 (left plot) and index 3 (right plot) (see Table I) for $\sqrt{s_{NN}} = 3$ GeV Au+Au collisions at 10–40 % centrality. The experimental measurements and the JAM (mean-field)+coalescence calculations of v_1 for each light nucleus are taken from Ref. [28].
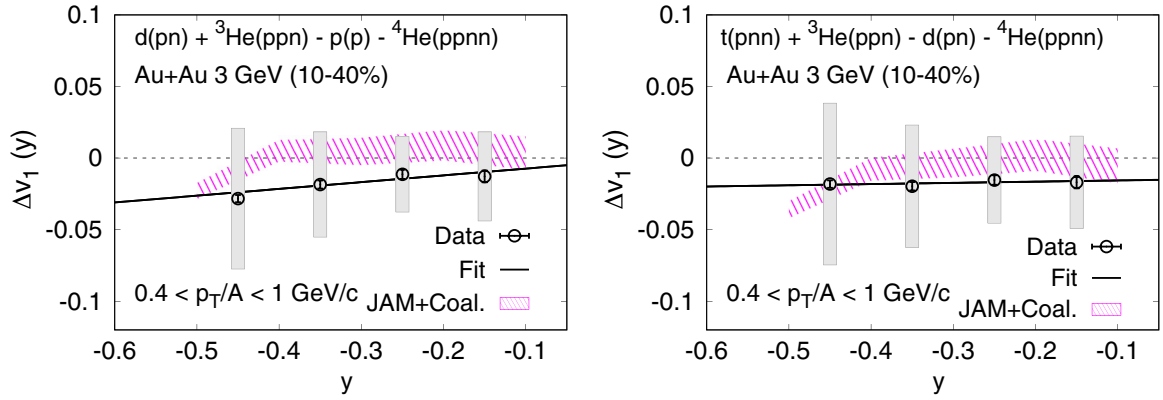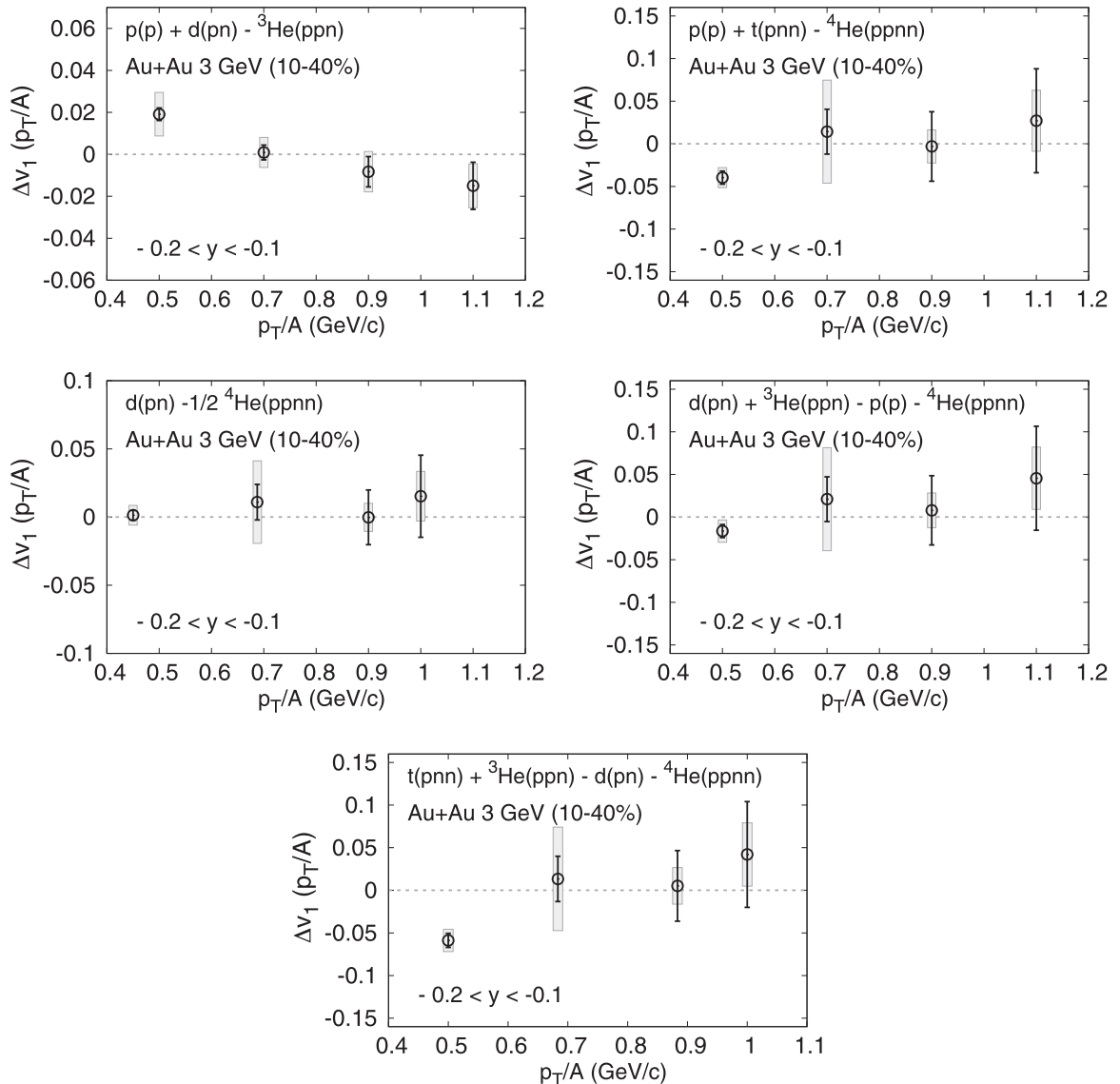
FIG. 3. Δv_1 based on index 4 (left plot) and index 5 (right plot) (see Table I) for $\sqrt{s_{NN}} = 3$ GeV Au+Au collisions at 10–40 % centrality. The experimental measurements and the JAM (mean-field)+coalescence calculations of v_1 for each light nucleus are taken from Ref. [28].

FIG. 4. Δv_1 as a function of p_T/A for indices 1–5 of Table I in $\sqrt{s_{NN}} = 3$ GeV Au+Au collisions at 10–40 % centrality. The calculations are made in the rapidity region, $-0.2 < y < -0.1$. The experimental measurements v_1 for each light nucleus are taken from Ref. [28].
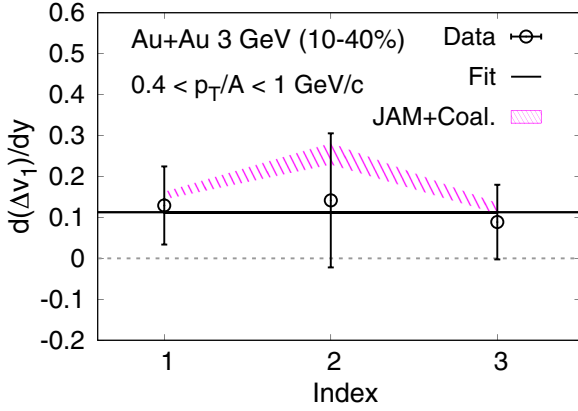
FIG. 5. Estimated Δv_1 slope ($d\Delta v_1/dy$) for indices 1, 2, and 3 (see Table I) in Au+Au collisions at $\sqrt{s_{NN}} = 3$ GeV for 10–40 % centrality.

Figure 2 presents Δv_1 as a function of y for index 2 and index 3 of Table I, based on the STAR measurements [28] for v_1 of light nuclei at $0.4 < p_T/A < 1$ GeV/c in $\sqrt{s_{NN}} = 3$ GeV Au+Au collisions at 10–40 % centrality. It is observed that Δv_1 is again consistent with zero near midrapidity, $-0.3 < y < 0$, within the measured uncertainties for both indices. The magnitudes of Δv_1 increase as the rapidity magnitude increases, and show a significant deviation from zero, in particular at larger rapidity magnitudes ($y < -0.3$). Nevertheless, the experimental errors are quite large, especially away from midrapidity. The JAM mean-field with coalescence calculations are consistent with the experimental data within uncertainties. The systematic deviation of Δv_1 from zero at large rapidity magnitude suggests a breakdown of the sum rule. Recently, the STAR Collaboration has found that v_1/A for all light nuclei, including protons, approximately follows A scaling near midrapidity, $-0.3 < y < 0$, and the scaling behavior worsens at $-0.4 < y < -0.3$ [28]. The model calculations are consistent with these findings from STAR.

Indices 4 and 5 of Table I have also been evaluated as a function of y in 10–40 % centrality Au+Au collisions at $\sqrt{s_{NN}} = 3$ GeV, as presented in Fig. 3. All data correspond to the same $y - p_T/A$ region: $-0.5 < y < 0$ and

$0.4 < p_T/A < 1$ GeV/c. It is seen here that Δv_1 is close to zero within errors for all rapidity bins. The current calculations have quite a large uncertainty, particularly at the larger rapidity magnitudes.

Exploration of all the indices of Table I in p_T space is very interesting. Figure 4 shows the p_T/A dependence of Δv_1 for indices 1–5 in 10–40 % centrality Au+Au collisions at $\sqrt{s_{NN}} = 3$ GeV. The calculations are made in the rapidity region, $-0.2 < y < -0.1$. The calculated Δv_1 with p_T/A is close to zero within the available experimental uncertainties. Nevertheless, the data point in $0.4 < p_T/A < 0.6$ GeV/c is a little away from zero for Index 2 and 5, and it requires further attention. It is clear that the sum rule for light nuclei is approximately valid near midrapidity when investigated in p_T space as well.

Magnitudes of v_1 become larger at larger rapidity magnitudes. Beam fragments from the target rapidity region ($y < -1.045$, for $\sqrt{s_{NN}} = 3$ GeV Au+Au collisions) can be transported to the hot collision zone and the produced medium might be contaminated. Fragment contamination increases at larger rapidity magnitudes and plays a role in determining the flow of produced light nuclei. Since the fragments suffer hard interactions and more of them while being transported to the collision zone, they have different v_1 than a nucleon produced in the collision. The fragment contribution to light nuclei formation is likely to be greater in the region of larger rapidity magnitude and hence a simple coalescence-inspired sum rule might be less valid there.

Only Δv_1 for index 1–5 of Table I have been discussed so far. The other two indices (index 6 and 7) contain hydrogen hypernuclei ($^3_\Lambda$H and $^4_\Lambda$H) and v_1 measurements for these species are not yet available. Based on index 6 and 7, the v_1 for $^3_\Lambda$H and $^4_\Lambda$H in $\sqrt{s_{NN}} = 3$ GeV Au+Au collisions are predicted in the present work.

The slopes $\Delta v_1(y)$ ($d\Delta v_1/dy$) for indices 1–5 of Table I are evaluated for Au+Au collisions at $\sqrt{s_{NN}} = 3$ GeV at 10–40 % centrality. In the ideal case where the sum rule holds, $d\Delta v_1/dy$ for all indices should be zero. Hence, the deviation of $d\Delta v_1/dy$ from zero is a measure of the sum rule violation. In Fig. 5, $d\Delta v_1/dy$ is shown for three linearly independent indices, namely 1, 2, and 3 of Table I. The JAM mean-field with coalescence calculations also show similar behavior. The
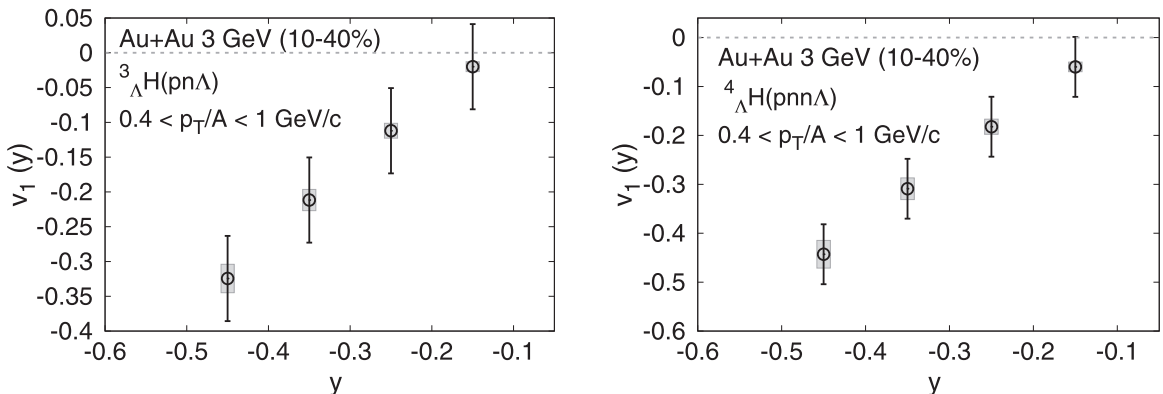

FIG. 6. Data-driven predictions of v_1 of hypernuclei $^3_\Lambda$H (left plot) and $^4_\Lambda$H (right plot) for $\sqrt{s_{NN}} = 3$ GeV Au+Au collisions at 10–40 % centrality. The predictions use index 6 and 7 of Table I, with the v_1 values taken from STAR measurements [28].
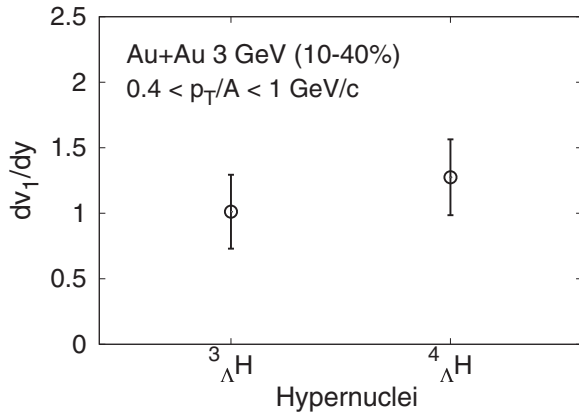
FIG. 7. Data-driven predictions of v_1 slope (dv_1/dy) for the hypernuclei ${}_{\Lambda}^{3}$H and ${}_{\Lambda}^{4}$H from $\sqrt{s_{NN}} = 3$ GeV Au+Au collisions at 10–40 % centrality.

reason to report $d\Delta v_1/dy$ only for independent indices is to fit the independent points to extract a global trend of the deviation of the calculated Δv_1 slope from zero. A constant fit of $d\Delta v_1/dy$ in Fig. 5 yields $C = 0.15 \pm 0.007$. This is an overall measure of the sum rule violation, and has been taken into account in the present data-driven prediction of v_1 for hypernuclei ${}_{\Lambda}^{3}$H and ${}_{\Lambda}^{4}$H from $\sqrt{s_{NN}} = 3$ GeV Au+Au collisions.

Figure 6 reports predictions of v_1 for hypernuclei ${}_{\Lambda}^{3}$H and ${}_{\Lambda}^{4}$H in the reduced transverse momentum range $0.4 < p_T/A < 1$ GeV/c in $\sqrt{s_{NN}} = 3$ GeV Au+Au collisions at 10–40 % centrality. The predictions are derived from Eqs. (4) and (5) in a model-independent way, i.e., the terms in these equations are taken from STAR measurements [28,43].

The predicted v_1 slope (dv_1/dy) for ${}_{\Lambda}^{3}$H and ${}_{\Lambda}^{4}$H at $0.4 < p_T/A < 1$ GeV/c from $\sqrt{s_{NN}} = 3$ GeV 10–40 % central Au+Au collisions is reported in Fig. 7. The v_1 slopes are obtained by fitting the data-driven results for ${}_{\Lambda}^{3}$H and ${}_{\Lambda}^{4}$H as shown in Fig. 6. The extracted slope values are dv_1/dy (${}_{\Lambda}^{3}$H) $= 1.012 \pm 0.282$ and dv_1/dy (${}_{\Lambda}^{4}$H) $= 1.274 \pm 0.289$. The STAR Collaboration has already collected large data samples that will provide greatly increased statistics for hypernuclei. Current predictions of v_1 and dv_1/dy for ${}_{\Lambda}^{3}$H and ${}_{\Lambda}^{4}$H will serve as a baseline for ongoing and future measurements.

IV. SUMMARY

Light nuclei and hypernuclei carry important information on the collective motion of the produced nuclear matter in heavy-ion collisions. However, their production mechanism remains uncertain. Light nuclei and hypernuclei can be formed by coalescence of nucleons and Λ hyperons, which are close to each other in both coordinate and momentum space. Atomic mass number scaling for light nuclei, a consequence of the coalescence mechanism, is found to hold approximately near midrapidity, whereas departures from this scaling behavior appear to occur, with marginal statistical significance, away from midrapidity [28]. This traditional scaling pattern involves dividing the anisotropic flow coefficients of a light nucleus or hypernucleus by its number of constituent baryons. This scaling ignores the mass and charge differences among the constituents, which can be expected to influence the coalescence mechanism. In this paper, an approach is discussed to test the coalescence-inspired sum rule for light nuclei and hypernuclei in a data-driven way, where each constituent is balanced appropriately in terms of mass and charge. In this approach, various light nuclei and hypernuclei are combined, and then the combinations having identical constituents are compared, i.e., comparisons are made for the same mass and same charge at the constituent level. The method is applied to STAR flow measurements for light nuclei from $\sqrt{s_{NN}} = 3$ GeV Au+Au collisions. It is observed that the sum rule is valid approximately near midrapidity, $-0.3 < y < 0$, and it is violated away from midrapidity, $y < -0.3$, with 1.84σ statistical significance. The JAM mean-field with coalescence calculations also are consistent with the data-driven results. There is an overall consistency between the calculations presented here regarding the sum rule and STAR findings on A scaling for light nuclei. The v_1 of hypernuclei ${}_{\Lambda}^{3}$H and ${}_{\Lambda}^{4}$H is predicted in a data-driven way over a reduced transverse momentum range $0.4 < p_T/A < 1$ GeV/c for $\sqrt{s_{NN}} = 3$ GeV Au+Au collisions at 10–40 % centrality. The predicted v_1 slope is $dv_1/dy = 1.012 \pm 0.282$ and 1.274 ± 0.289 for ${}_{\Lambda}^{3}$H and ${}_{\Lambda}^{4}$H, respectively. The STAR Collaboration has acquired large data samples that will provide greatly increased statistics for hypernuclei over a range of collision energies. The current predictions will serve as a baseline for these upcoming hypernuclear v_1 measurements.

[1] S. Voloshin and Y. Zhang, Flow study in relativistic nuclear collisions by Fourier expansion of Azimuthal particle distributions, Z. Phys. C **70**, 665 (1996).

[2] A. M. Poskanzer and S. A. Voloshin, Methods for analyzing anisotropic flow in relativistic nuclear collisions, Phys. Rev. C **58**, 1671 (1998).

[3] U. Heinz and R. Snellings, Collective flow and viscosity in relativistic heavy-ion collisions, Annu. Rev. Nucl. Part. Sci. **63**, 123 (2013).

[4] P. Danielewicz, R. Lacey, and W. G. Lynch, Determination of the equation of state of dense matter, Science **298**, 1592 (2002).

[5] J. Adams et al. (STAR Collaboration), Directed flow in Au+Au collisions at s(NN)**(1/2) = 62-GeV, Phys. Rev. C **73**, 034903 (2006).

[6] B. I. Abelev et al. (STAR Collaboration), System-Size Independence of Directed Flow Measured at the BNL Relativistic Heavy-Ion Collider, Phys. Rev. Lett. **101**, 252301 (2008).

[7] L. Adamczyk *et al.* (STAR Collaboration), Directed Flow of Identified Particles in Au + Au Collisions at $\sqrt{s_N N} = 200$ GeV at RHIC, Phys. Rev. Lett. **108**, 202301 (2012).

[8] L. Adamczyk *et al.* (STAR Collaboration), Beam-Energy Dependence of the Directed Flow of Protons, Antiprotons, and Pions in Au+Au Collisions, Phys. Rev. Lett. **112**, 162301 (2014).

[9] L. Adamczyk *et al.* (STAR Collaboration), Beam-Energy Dependence of Directed Flow of Λ, $\bar{\Lambda}$, $K^{\pm}$, K_s^0 and ϕ in Au+Au Collisions, Phys. Rev. Lett. **120**, 062301 (2018).

[10] K. Aamodt *et al.* (ALICE Collaboration), Elliptic Flow of Charged Particles in Pb-Pb Collisions at 2.76 TeV, Phys. Rev. Lett. **105**, 252302 (2010).

[11] S. Acharya *et al.* (ALICE Collaboration), Probing the Effects of Strong Electromagnetic Fields with Charge-Dependent Directed Flow in Pb-Pb Collisions at the LHC, Phys. Rev. Lett. **125**, 022301 (2020).

[12] M. Abdallah *et al.* (STAR Collaboration), Measurements of HΛ3 and HΛ4 Lifetimes and Yields in Au+Au Collisions in the High Baryon Density Region, Phys. Rev. Lett. **128**, 202301 (2022).

[13] J. Adam *et al.* (STAR Collaboration), Measurement of the mass difference and the binding energy of the hypertriton and antihypertriton, Nature Phys. **16**, 409 (2020).

[14] L. Adamczyk *et al.* (STAR Collaboration), Measurement of the $^3_\Lambda$H lifetime in Au+Au collisions at the BNL Relativistic Heavy Ion Collider, Phys. Rev. C **97**, 054909 (2018).

[15] J. Adam *et al.* (ALICE Collaboration), $^3_\Lambda$H and $^3_{\bar{\Lambda}}\overline{\text{H}}$ production in Pb-Pb collisions at $\sqrt{s_{\text{NN}}} = 2.76$ TeV, Phys. Lett. B **754**, 360 (2016).

[16] B. I. Abelev *et al.* (STAR Collaboration), Observation of an antimatter hypernucleus, Science **328**, 58 (2010).

[17] S. Acharya *et al.* (ALICE Collaboration), Elliptic and triangular flow of (anti)deuterons in Pb-Pb collisions at $\sqrt{s_{\text{NN}}} = 5.02$ TeV, Phys. Rev. C **102**, 055203 (2020).

[18] S. Acharya *et al.* (ALICE Collaboration), Measurement of deuteron spectra and elliptic flow in Pb–Pb collisions at $\sqrt{s_{\text{NN}}} = 2.76$ TeV at the LHC, Eur. Phys. J. C **77**, 658 (2017).

[19] M. D. Partlan *et al.* (EOS Collaboration), Fragment Flow in Au + Au Collisions, Phys. Rev. Lett. **75**, 2100 (1995).

[20] J. Barrette *et al.* (E877 Collaboration), Directed flow of light nuclei in Au+Au collisions at 10.8A GeV/c, Phys. Rev. C **59**, 884 (1999).

[21] G. Stoicea *et al.* (FOPI Collaboration), Azimuthal Dependence of Collective Expansion for Symmetric Heavy-Ion Collisions, Phys. Rev. Lett. **92**, 072303 (2004).

[22] W. Reisdorf *et al.* (FOPI Collaboration), Systematics of azimuthal asymmetries in heavy ion collisions in the 1 A GeV regime, Nucl. Phys. A **876**, 1 (2012).

[23] J. Adam *et al.* (STAR Collaboration), Beam-energy dependence of the directed flow of deuterons in Au+Au collisions, Phys. Rev. C **102**, 044906 (2020).

[24] L. Adamczyk *et al.* (STAR Collaboration), Measurement of elliptic flow of light nuclei at $\sqrt{s_{\text{NN}}} = 200$, 62.4, 39, 27, 19.6, 11.5, and 7.7 GeV at the BNL Relativistic Heavy Ion Collider, Phys. Rev. C **94**, 034908 (2016).

[25] J. Adamczewski-Musch *et al.* (HADES Collaboration), Directed, Elliptic, and Higher Order Flow Harmonics of Protons, Deuterons, and Tritons in Au + Au Collisions at $\sqrt{s_{\text{NN}}} = 2.4$ GeV, Phys. Rev. Lett. **125**, 262301 (2020).

[26] S. Acharya *et al.* (ALICE Collaboration), Production of deuterons, tritons, ^{3}He nuclei and their antinuclei in pp collisions at $\sqrt{s} = 0.9$, 2.76 and 7 TeV, Phys. Rev. C **97**, 024615 (2018).

[27] S. Wang *et al.* (EOS Collaboration), Light Fragment Production and Power Law Behavior in Au + Au Collisions, Phys. Rev. Lett. **74**, 2646 (1995).

[28] M. Abdallah *et al.* (STAR Collaboration), Light nuclei collectivity from sNN = 3 GeV Au+Au collisions at RHIC, Phys. Lett. B **827**, 136941 (2022).

[29] A. Andronic, P. Braun-Munzinger, K. Redlich, and J. Stachel, Decoding the phase structure of QCD via particle production at high energy, Nature (London) **561**, 321 (2018).

[30] V. Vovchenko and H. Stoecker, Examination of the sensitivity of the thermal fits to heavy-ion hadron yield data to the modeling of the eigenvolume interactions, Phys. Rev. C **95**, 044904 (2017).

[31] A. Andronic, P. Braun-Munzinger, J. Stachel, and H. Stocker, Production of light nuclei, hypernuclei and their antiparticles in relativistic nuclear collisions, Phys. Lett. B **697**, 203 (2011).

[32] W. Zhao, L. Zhu, H. Zheng, C. M. Ko, and H. Song, Spectra and flow of light nuclei in relativistic heavy ion collisions at energies available at the BNL Relativistic Heavy Ion Collider and at the CERN Large Hadron Collider, Phys. Rev. C **98**, 054905 (2018).

[33] D. Oliinychenko, L.-G. Pang, H. Elfner, and V. Koch, Microscopic study of deuteron production in PbPb collisions at $\sqrt{s} = 2.76$ TeV via hydrodynamics and a hadronic afterburner, Phys. Rev. C **99**, 044907 (2019).

[34] S. T. Butler and C. A. Pearson, Deuterons from High-Energy Proton Bombardment of Matter, Phys. Rev. Lett. **7**, 69 (1961).

[35] H. Sato and K. Yazaki, On the coalescence model for high-energy nuclear reactions, Phys. Lett. B **98**, 153 (1981).

[36] S. Zhang, J. H. Chen, H. Crawford, D. Keane, Y. G. Ma, and Z. B. Xu, Searching for onset of deconfinement via hypernuclei and baryon-strangeness correlations, Phys. Lett. B **684**, 224 (2010).

[37] Y. Nara, N. Otuka, A. Ohnishi, K. Niita, and S. Chiba, Study of relativistic nuclear collisions at AGS energies from p + Be to Au + Au with hadronic cascade model, Phys. Rev. C **61**, 024901 (1999).

[38] M. Isse, A. Ohnishi, N. Otuka, P. K. Sahu, and Y. Nara, Mean-field effects on collective flows in high-energy heavy-ion collisions from AGS to SPS energies, Phys. Rev. C **72**, 064908 (2005).

[39] The STAR Beam Use Request For Run 21, https://drupal.star.bnl.gov/STAR/files/BUR2020_final.pdf, accessed: 2021-09-21.

[40] A. I. Sheikh, D. Keane, and P. Tribedy, Testing the impact of electromagnetic fields on the directed flow of constituent quarks in heavy-ion collisions, Phys. Rev. C **105**, 014912 (2022).

[41] K. F. Riley, M. P. Hobson, and S. J. Bence, *Mathematical Methods for Physics and Engineering: A Comprehensive Guide* (Cambridge University Press, Cambridge, 2006).

[42] S. Sombun, K. Tomuang, A. Limphirat, P. Hillmann, C. Herold, J. Steinheimer, Y. Yan, and M. Bleicher, Deuteron production from phase-space coalescence in the UrQMD approach, Phys. Rev. C **99**, 014901 (2019).

[43] M. S. Abdallah *et al.* (STAR Collaboration), Disappearance of partonic collectivity in sNN = 3GeV Au+Au collisions at RHIC, Phys. Lett. B **827**, 137003 (2022).